Applied Catalysis B: Environmental 227 (2018) 170–177

Contents lists available at ScienceDirect

Applied Catalysis B: Environmental

journal homepage: www.elsevier.com/locate/apcatb

On the performance of HOCl/Fe^{2+}, HOCl/Fe^{2+}/UVA, and HOCl/UVC processes using *in situ* electrogenerated active chlorine to mineralize the herbicide picloram

Douglas A.C. Coledam[a,1], Isaac Sánchez-Montes[a,1], Bianca F. Silva[b], José M. Aquino[a,*]

[a] Universidade Federal de São Carlos, Departamento de Química, 13565-905 São Carlos, SP, Brazil
[b] Universidade Estadual Paulista, Instituto de Química de Araraquara, Departamento de Química Analítica, 14800-900 Araraquara, SP, Brazil

ARTICLE INFO

Keywords:
Fenton like reaction
Synthetic organic pollutants
Organochlorine compounds
Mixed oxide anode
Hybrid methods

ABSTRACT

Four different treatment methods based on the HO· production were assessed to oxidize and mineralize the herbicide picloram (PCL), which is considered very toxic and so is a potential contaminant of surface and ground water. The processes based on the Fenton type (homolysis reaction of HOCl by Fe^{2+} ions) and photo-Fenton type reaction (using a 9 W UVA light) with *in situ* electrogenerated HOCl species, using a commercial DSA® anode in the presence of Cl^- ions, led to poor mineralization performances in comparison to the HOCl/UVC process. In that case, the homolysis reaction of HOCl mediated by a 5 or 9 W UVC light resulted in almost complete removal of the organic load within 12 h of treatment, from acidic to neutral solutions and using 1 g L^{-1} of NaCl concentration after optimization of the experimental conditions. When the HOCl/UVC process using a 5 W UVC light is compared to the electrochemical method using a boron-doped diamond anode (electrochemical/BDD), the oxidation and mineralization rates of the HOCl/UVC process were always superior, with ~95% removal of total organic carbon (TOC) after 12 h treatment. The energy consumption per unit mass of removed TOC remained around 4 and 8 kW h g^{-1} for the HOCl/UVC and electrochemical/BDD treatment processes after 90% removal of TOC, respectively, even considering the energy consumption of the UVC lamp. In the final treatment stages, high CO_2 conversions were obtained using both methods, as the generated intermediates were almost completely eliminated. Finally, the HOCl/UVC process is a reasonable option to treat solutions contaminated with organic pollutants as the common problems associated with the Fenton based (acidic solution, Fe^{2+} ion recovery, generation of H_2O_2) and electrochemical/BDD (mass transport) processes can be readily circumvented.

1. Introduction

The contamination of surface natural water bodies by a large number of synthetic organic compounds (SOC) seems to be reported more frequently by the literature [1–3] nowadays, since feed water supply systems usually use surface water [3]. These studies have shown that SOC, such as herbicides, antibiotics, personal care products, and so on [4,5], can be found in natural surface water even after treatment at conventional municipal wastewater treatment plants [6,7]. Despite a significant number of studies that show the impact of the acute toxicity of some SOC on microorganisms [8,9], including the relationship between toxicity and structural modifications [10–12], few of these studies investigated the effect of a long term exposure of SOC in microorganisms or even in humans. Consequently, and based on the potential harmful effect of SOC to aquatic and human lives [13], there is the necessity to adequately eliminate these pollutants presented on effluents, using distinct methods or their combination [14], before disposal in the environment.

Among the available methods to treat effluents contaminated with SOC, the ones based on generation of the non selective hydroxyl radicals (HO·) are usually the choice, such as Fenton based [15] and electrochemical processes [16] as well as their combination [17], due to the high oxidation power of HO· and production of less toxic by-products [10]. The necessity to use acidic solutions and recovery of Fe^{2+} ions are the main drawback of the Fenton based processes. On the other hand, mass transfer limitation and the choice of adequate electrode materials limit the application of the electrochemical technology, resulting in excessive energy expenses and limited space-time yields [18]. In order to try to overcome these limitations, considering the solution pH, mass transfer limitation and anode material, Fenton type

* Corresponding author.
E-mail address: jmaquino@ufscar.br (J.M. Aquino).
[1] These authors contributed equally to this work.

https://doi.org/10.1016/j.apcatb.2017.12.072
Received 12 October 2017; Received in revised form 25 December 2017; Accepted 30 December 2017
Available online 01 January 2018
0926-3373/

based reactions (particularly the reaction between HOCl and Fe^{2+} ions) have been proposed [19] and seems to be an alternative process [20,21] to treat solutions contaminated with organic compounds, as also recently shown by Brillas and coworkers [22]. A Fenton type reaction is based on the homolysis reaction of the HOCl species (electrochemically produced using mixed oxide anodes or added as a chemical reagent) by Fe^{2+} ions (or other Fe^{2+} complex ion [23]) to produced HO· and Cl· species. The process performance can be increased if a suitable combination of the electrochemical and photochemical (using a UVA light to eliminate Fe complexes with carboxylic acids [24]) methods are carried out [22].

The use of active chlorine species (HOCl and OCl^-) to oxidize SOC was also investigated in many works in the literature [25,26], specifically when using the electrochemical technology, as those species lead to an indirect oxidation pathway in the solution bulk; however, due to the low oxidation power of active chlorine species that often lead to addition reactions in organic molecules [27], resulting in poor mineralization levels and generation of organochlorine byproducts are often reported as the main drawbacks. Some strategies to overcome these difficulties were proposed such as the photo-assisted methods [28]; however, the use of high power UVC lamps (high electrical energy consumption) to irradiate dimensionally stable anode (DSA®) surfaces in order to promote the formation of the HO· species, through oxidation of adsorbed H_2O by the produced holes, were inefficient to mineralize SOC. Recently, Hurwitz et al. [29] and Sánchez-Montes et al. [30] showed that the photo-assisted method could be successfully rearranged (by the elimination of the heterogeneous photocatalysis reaction) to promote the homolysis of the *in situ* electrogenerated active chlorine species using low power UVC lamps (also called hybrid electrochemical and photochemical process), in the solution bulk. Despite the production of organochlorine byproducts during treatment of the tebuthiuron herbicide [30], in the final stages of the electrochemical and photochemical treatment, no such oxidation byproducts were detected.

Thus, the aim of the present work is to compare the performances of the Fenton type reaction in the absence (HOCl/Fe^{2+} process) and presence (photo-Fenton type process or HOCl/Fe^{2+}/UVA process) of a low power UVA light and using *in situ* electrogenerated active chlorine species (particularly HOCl) produced by a commercially available DSA® type electrode during degradation of the picloram (PCL: 4-Amino-3,5,6-trichloro-2-pyridinecarboxylic acid) herbicide. This compound, which is derived from a pyridine ring, has been extensively used and investigated [31–34] worldwide and is considered very toxic by the Brazilian Health Regulatory Agency. In addition, the performance of an electrochemical and photochemical process, through homolysis of the HOCl species using a low power UVC light, is intended to be compared with the Fenton type processes. The comparison will be carried out using a filter press flow cell and the investigated variables will be the type of UV irradiation, solution pH and NaCl concentration. The assessment of PCL degradation and its produced intermediates will be carried out by high performance liquid chromatography coupled to mass spectrometry analyses. The optimized results considering the investigated processes and their variables, as well as the mineralization current efficiency, electrical energy consumption, and extent of total electrochemical combustion (conversion to CO_2) will be compared to those attained using solely the electrochemical method with a boron-doped diamond (BDD) anode in the same hydrodynamic conditions. Finally, it is intended to compare the oxidation and mineralization efficiency of a model organic compound based on three catalytic reactions to produce HO·: homolysis reaction mediated by Fe^{2+} ions or UVC irradiation and from water discharge.

2. Experimental

2.1. Chemicals

All chemicals, including picloram (PCL: 240 g L^{-1}, as a salt of triethanolamine – $C_6H_{15}NO_3$; the rest of the formulation is referred to as inert ingredients, except the crystal violet dye – $C_{25}N_3H_{30}Cl$, Adama Brasil), Na_2SO_4 (a.r., Qhemis), NaCl (a.r., Qhemis), $Na_2S_2O_3$ (a.r., Qhemis), KI (a.r., Synth), H_3PO_4 (85%, Mallinckrodt), $Na_2S_2O_8$ (a.r., Sigma Aldrich), KSCN (a.r., Merck), NaOH (a.r., Synth), H_2SO_4 (a.r., Mallinckrodt), $Na_2[Fe(CN)_5NO]{\cdot}2H_2O$ (a.r., Fisher company), Na_2CO_3 (a.r., Sigma Aldrich), $NaHCO_3$ (a.r., Sigma Aldrich), benzoic acid (a.r., Sigma Aldrich), salicylic acid (a.r., Sigma Aldrich), 1,10-phenanthroline (a.r., Sigma Aldrich), hydroxylamine hydrochloride (a.r., Sigma Aldrich), formic acid (a.r., JT Baker) and acetonitrile (HPLC grade, JT Baker), were used as received. All analyzed carboxylic acids were purchased from Sigma Aldrich. Deionized water (Millipore Milli-Q system, resistivity ≥18.2 MΩ cm) was used for the preparation of all solutions.

2.2. Electrochemical and photochemical degradation experiments

A schematic representation of the electrochemical and photochemical flow system, as well as the one-compartment filter-press flow reactor (containing a DSA® – $Ti/Ru_{0.3}Ti_{0.7}O_2$ of nominal composition) and two AISI 304 stainless steel plates as anode and cathodes, respectively, used during the PCL degradation experiments can be seen in a previous work [30]. The exposed area of the DSA® anode was 4.16 cm × 2.75 cm (each face), respectively, and the distance between electrodes was around 5 mm.

In the first part of this work, the assessment of the HOCl/Fe^{2+} and HOCl/Fe^{2+}/UVA processes were carried out by the *in situ* electrochemical generation of HOCl species (using 20 mA cm^{-2}, at pH 3, and with 2 g L^{-1} NaCl) in the presence of varying amounts of initial Fe^{2+} ion concentrations ($[Fe^{2+}]_0$: 0, 0.5, 1.0, and 2.0 mmol L^{-1}) and using or not a 9 W UVA lamp. Then, in the second part, during assessment of the HOCl/UVC process, the investigated variables and their ranges were: *i*) power of commercial UVC lamps (5 and 9 W), *ii*) solution pH (3, 7, 11, and without control), and *iii*) NaCl concentration (0, 1, 2, and 4 g L^{-1}). The solution pH was continuously monitored and kept constant at the desired values by addition of concentrated solutions of H_2SO_4 or NaOH. The fluency rate of the UVA and UVC lamps as well as their corresponding emission spectra were measured with a Nova radiometer and spectroradiometer (from Ophir) and the obtained values can be seen in Table SM-1 and in Fig. SM-1, respectively, in the supplementary material file. The PCL concentration, type and concentration of the supporting electrolyte, flow rate (flow velocity), electrolysis time, and treated solution volume were fixed at 100 mg L^{-1}, 0.1 mol L^{-1} Na_2SO_4, 420 L h^{-1} (0.3 m s^{-1}), 360 min, and 1.0 L, respectively. Before any electrochemical and photochemical experiment and in order to eliminate any adsorbed organic compound on the DSA® surface, this electrode was electrochemically pretreated using a 0.1 mol L^{-1} Na_2SO_4 solution by applying 20 mA cm^{-2} for 15 min.

After optimization of the electrochemical and photochemical process using the UVC lamp (HOCl/UVC process), its performance towards degradation of PCL (concerning removal of the dissolved organic matter and electrical energy efficiency) were compared to the electrochemical method using a BDD anode and similar hydrodynamic parameters concerning the surface to volume ratio (24 cm^2 of geometric area) and flow velocity (0.3 m s^{-1}: see [10] for more details of the electrochemical cell setup). The BDD electrode (boron content of 500 ppm in the BDD film, deposited on a Si substrate) was purchased from NeoCoat SA (Switzerland).

2.3. Analyses

The evolution of the PCL concentration was monitored by high performance liquid chromatography (HPLC) using a core shell C-18 reversed phase as the stationary phase (150 mm × 4.6 mm, 5 µm particle size, from Phenomenex®) and a mixture of H_2O and acetonitrile (75:25 *V/V*) in an isocratic elution mode as the mobile phase, at 1 mL min^{-1}. The PCL molecule was detected at 254 nm. The injection volume and temperature of the column were 25 µL and 23 °C, respectively.

Analyses of the intermediate compounds were made every 1 h until 8 h of electrolysis. The 2 mL extracted samples were first frozen and then dried in a lyophilization system (CHRIST alpha 2–4 LD Plus) for 24 h. After this period, the samples were resuspended in 1 mL of acetonitrile and filtered using a 0.22 µm cartridge coupled to a glass syringe. The intermediates formed during the PCL degradation process were determined by liquid chromatography coupled to a mass spectrometer (LC–MS/MS) analyses, according to a methodology previously described [30]. During MS/MS experiments, formic acid was added in the H_2O component of the mobile phase to attain a final concentration of 0.1% (*V/V*). The injection volume was 20 µL.

Short chain carboxylic acids were also determined throughout the electrolysis process by HPLC, using a Rezek ROA-H™ column from Phenomenex® as the stationary phase and 2.5 mmol L^{-1} H_2SO_4 as the mobile phase at 0.5 mL min^{-1}. The carboxylic acids (detected at 210 nm) were identified by the comparison of their retention times with those of previously analyzed standards. The injection volume and column temperature were maintained at 25 µL and 23 °C, respectively.

Iodometric titration was used to monitor the amount of electrogenerated active chlorine species (calculated as Cl_2), according to a standard method [35].

Total Fe concentration were determined by UV–vis spectroscopy using the Phenanthroline method [35], after a previous treatment of samples using a concentrated hydroxylamine hydrochloride solution. The Fe^{2+} ion concentration was obtained by a simple mass balance after quantification of Fe^{3+} ions using a stock solution of KSCN. The NH_4^+ ions were also quantified by UV–vis spectroscopy based on the production of indophenol (phenate method [35]). Ion chromatography (930 Compact IC flex from Metrohm) were carried out to determine the concentration evolution of NO_3^- ions using a Metrosep A Supp5–250/4.0 column and a mixture of 3.2 mmol L^{-1} Na_2CO_3 and 1.0 mmol L^{-1} $NaHCO_3$ as the stationary and mobile phase, respectively. The injection volume and flow rate were kept fixed at 50 µL and 0.7 mL min^{-1}. A conductivity detector was used to identify different produced ions.

A GE Sievers Innovox analyzer was used to monitor the extent of mineralization (*i.e.* conversion to CO_2) by total organic carbon concentration ([TOC]) measurements. For such, the treated solution was sampled (5 mL) every 1 h. The [TOC] determination was carried out after mixing a diluted volume of the treated sample with H_3PO_4 (6 mol L^{-1}) and $Na_2S_2O_8$ (30% *m/V*) solutions. The sample oxidation was accomplished after the temperature and pressure corresponding to the supercritical point of water was reached. The TOC content was analyzed by subtraction of the measured values of inorganic and total carbon, in terms of generated CO_2. More experimental details can be found in previous works of our group [10,30].

The mineralization current efficiency (*MCE*) was calculated according to the following equation [36]:

$$MCE = \frac{\Delta[\mathrm{TOC}]_t nFV}{4.32 \times 10^7 mIt} \times 100 \quad (1)$$

where $\Delta[TOC]_t$ is the measured TOC removal (mg L^{-1}) after a certain treatment time, *t* (h), *n* the number of exchanged electrons (see Eq. (2) and assuming that only NO_3^- ions are produced [37]) considering that the applied electric charge was consumed solely by the mineralization process, *F* the Faraday constant (96485C mol^{-1}), *V* the solution volume (L), 4.32×10^7 is a compounded conversion factor (3600 s h^{-1} × 12,000 mg mol^{-1}), *m* the number of carbon atoms of the PCL molecule, and *I* the applied electric current (A).

$$C_6H_3Cl_3N_2O_2(aq) + 16H_2O(l) \rightarrow 6CO_2(g) + 2NO_3^-(aq) + 3Cl^-(aq) + 35H^+(aq) + 30e^- \quad (2)$$

The extent of combustion (φ) [38] was calculated through the ratio between the removal percentages of PCL and TOC each 1 h of treatment:

$$\varphi = \frac{\%[\mathrm{TOC}]_{\mathrm{removed}}}{\%[\mathrm{PCL}]_{\mathrm{removed}}} \quad (3)$$

The value of φ gives an indication of the extent of conversion of oxidized PCL molecules to CO_2 or to other intermediate compounds. Then, this parameter can assume values between 0 (no combustion) and 1 (complete combustion, which is the desired value).

The energy consumption per unit mass (*w*) for the electrochemical and photochemical process was calculated according to [39]:

$$w = \left(\frac{UIt + Pt}{\Delta[X]V}\right) \quad (4)$$

where *U* is the cell voltage (V), *I* the applied electric current (A), *t* the reaction time (h), *P* the nominal power of the UVA/UVC lamps (W), Δ[X] the concentration variation of PCL (mg L^{-1}) or TOC (mg L^{-1}) after a certain treatment time, and *V* the solution volume (L).

3. Results and discussion

3.1. Assessment of the HOCl/Fe^{2+} and HOCl/Fe^{2+}/UVA processes

Fig. 1 shows the relative percentage decay of PCL ($[PCL]_{rel}/\% = 100 \times [PCL]_t/[PCL]_0$, where $[PCL]_t$ and $[PCL]_0$ refer to the PCL concentration after a certain time *t* and at the beginning of the treatment process, respectively) and TOC ($[TOC]_{rel}/\% = 100 \times [TOC]_t/[TOC]_0$, where $[TOC]_t$ and $[TOC]_0$ refer to the TOC concentration after a certain time *t* and at the beginning of the treatment process, respectively) as a function of treatment time (*t*) for the Fenton type process with *in situ* electrogenerated active chlorine species and using distinct initial concentrations of Fe^{2+} ($[Fe^{2+}]_0$: from 0 to 2 mmol L^{-1}). The oxidation levels attained for the PCL compound using the electrochemical method without Fe^{2+} ions was very close to the experiments in the presence of increasing amounts of Fe^{2+} ($k_{oxi} \sim 6 \times 10^{-2}$ min^{-1}). Thus, the main contribution for the oxidation of PCL is due to the electrochemical process that is mediated by the electrogenerated active

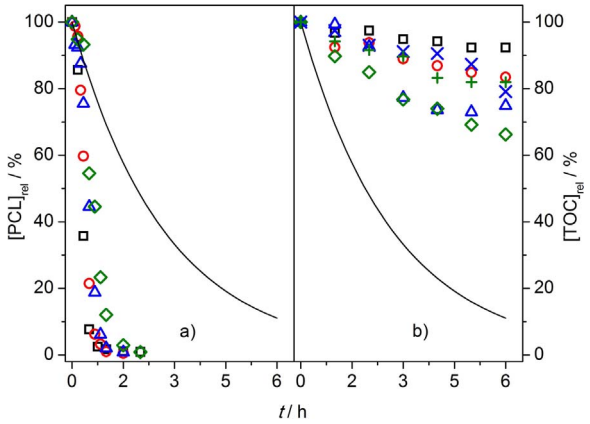

Fig. 1. Relative percentage decay of a) PCL ($[PCL]_{rel}$) and b) TOC ($[TOC]_{rel}$) as a function of treatment time for the Fenton type process (using a DSA® anode to electrogenerate active chlorine species) at varying initial concentration of Fe^{2+} ions: (◯) 0.0, (○) 0.5, (△ and its repetition ✕) 1.0, and (◇ and its repetition +) 2.0 mmol L^{-1} Fe^{2+} ions. Continuous line refer to a theoretical mass transport controlled process (see text). Conditions: 20 mA cm^{-2}, pH 3, 2 g L^{-1} NaCl, and at 25 °C.

chlorine species (particularly the HOCl specie in the investigated pH condition [40]), as often reported in the literature [33]. The indirect oxidation reaction increases the oxidation kinetic constant of organics in comparison to a purely mass transport controlled electrochemical reaction (in the absence of chemical reactions in the solution bulk) [41], as can be seen by comparison of the theoretical exponential line (obtained according to [42] and using 2.13×10^{-5} m and 9.1×10^{-10} m^2 s^{-1} for the thickness of the stagnant layer [43] and diffusion coefficient for PCL [44], respectively) and experimental data of Fig. 1. The expected synergistic reaction between Fe^{2+} ions and HOCl species to mainly generate HO· or Cl· (Fenton type or like Fenton reactions), as described in the work of Folkes et al. [19] and shown in Eqs. (5) and (6), seem to not result in significant improvements in the oxidation level or rate of the PCL compound. That behavior might be due to the faster oxidation reaction of the HOCl species towards the PCL molecule.

$$HOCl(aq) + Fe^{2+}(aq) \rightarrow Fe^{3+}(aq) + HO\cdot(aq) + Cl^{-}(aq) \quad (5)$$

$$HOCl(aq) + Fe^{2+}(aq) \rightarrow Fe^{3+}(aq) + HO^{-}(aq) + Cl\cdot(aq) \quad (6)$$

On the other hand, when the TOC decay is analyzed, the electrochemical process in the presence of Fe^{2+} ions resulted in increasing removal levels of TOC: ~35% (~20% for the repetition) of CO_2 conversion using 2 mmol L^{-1} Fe^{2+} ions in comparison to ~10% in the absence of Fe^{2+} ions. The expected synergism of the Fenton type reaction, probably due to the generation of HO· species [19] on the solution bulk, according to Eq. (5), can be clearly noticed. The production of HO· species were confirmed after detection of salicylic acid during treatment of a solution containing benzoic acid by the Fenton type reaction (see experimental details and results in the supplementary material section – Fig. SM-2a). In addition, the concentration evolution of Fe as a function of treatment time showed that during the Fenton type reaction, practically no Fe^{2+} ion accumulates in the reaction medium, since all detected Fe is in the oxidation state of +3 (see Fig. SM-3).

The use of UVA light (9 W) was also carried out to investigate the performance of the Fenton type reaction to oxidize and mineralize solutions containing the PCL herbicide. As reported in the literature for photo-Fenton processes, the irradiation of the treating solution with UVA light led to significant improvements in the oxidation and mineralization levels of organic pollutants due to regeneration of Fe^{2+} ions by elimination of its complexes with carboxylic acids or H_2O [45,46]. When Fenton type reactions are analyzed, it is interesting to observe a significant increase of the absorption bands from 200 nm to 350 nm, during analyses of UV–vis spectra of solutions in presence of HOCl and Fe^{2+} ions (without organic compounds), as shown in Fig. SM-5. As reported by Folkes et al. [19], that behavior might be related to the oxidation of Fe^{2+} ions to higher oxidation states or even complexation with Cl^{-} ions. Consequently, a photo-Fenton type process was carried out through irradiation of the solution with a 9 W UVA light to assess the performance of this method towards oxidation and mineralization of the PCL herbicide. As can be observed in Fig. 2, which shows the evolution of $[PCL]_{rel}$ and $[TOC]_{rel}$ for the photo-Fenton type process at varying amounts of $[Fe^{2+}]_0$ (from 0 to 2 mmol L^{-1}) upon irradiation by a 9 W UVA light with *in situ* electrogenerated active chlorine species, the PCL oxidation rates attained were very similar to the one without irradiation and Fe^{2+} ions (see Fig. 1a). Therefore, the PCL molecule reacts readily with active chlorine species through oxidation, substitution, or addition reactions [27], and no synergistic effect was observed. When conversion to CO_2 is analyzed, the removal levels and rates (see Table SM-2 for the pseudo first order kinetic constants) of TOC increased slightly for all tested concentrations of Fe^{2+} ions in comparison to the experiments without UVA irradiation (compare Figs. 1b and 2b): ~45% (35% to 25% for the repetitions) of CO_2 conversion using 1 or 2 mmol L^{-1} Fe^{2+} ions. These improvements might be due to the regeneration of the Fe^{2+} ions by the photoreduction processes

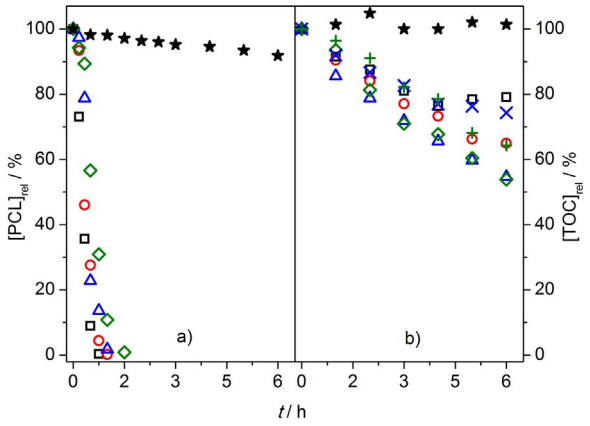

Fig. 2. Relative percentage decay of a) PCL ($[PCL]_{rel}$) and b) TOC ($[TOC]_{rel}$) as a function of treatment time for the photo-Fenton type process (using a 9 W UVA light and a DSA® anode to electrogenerate active chlorine species) at varying initial concentration of Fe^{2+} ions: (□) 0.0, (○) 0.5, (△ and its repetition ✕) 1.0, (◇ and its repetition +) 2.0 mmol L^{-1} Fe^{2+} ions, and (★) photochemical experiment. Conditions: 20 mA cm^{-2}, pH 3, 2 g L^{-1} NaCl, and at 25 °C.

mediated by UVA irradiation, as reported for photo-Fenton based reactions [45]. Then, the Fe^{2+} ions generate HO· by homolysis of the HOCl species, as shown in Fig. SM-2b. For comparison purposes, no significant oxidation or mineralization of PCL was attained using only the photochemical method (without applying electric current and no addition of Fe^{2+} ions) experiment. The synergistic effect of the photo-Fenton type process (despite the low reprodutibility) can be easily confirmed for the TOC removal process by summation of the removal levels of the electrochemical and photochemical methods and comparison with the experimental data, as shown in Fig. SM-6. Clearly, the experimental data of the photo-Fenton type reaction led to a slightly higher TOC removal.

The concentration evolution of Fe as a function of treatment time for the photo-Fenton type process can be seen in Fig. SM-7. As can be inferred from Fig. SM-7, no appreciable Fe^{2+} ion concentration was detected in the reaction medium. That behavior is in agreement with the Fenton type process and is due to the high concentration of electrogenerated active chlorine (see discussion and corresponding figures below) that promptly oxidizes Fe^{2+} to Fe^{3+} ions.

The extent of total electrochemical combustion (φ) and mineralization current efficiency (*MCE*) for the Fenton type and photo-Fenton type processes can be seen in Fig. SM-8. As expected, a slight increase of the φ values were noticed for the photo-Fenton type reaction; however, no significant differences were observed for the obtained *MCE* values. Further improvements in the conversion to CO_2 might be expected if a powerful UVA light had been used, such as the sunlight; however, due to experimental limitations concerning the assembled system, this was not feasible. Similar results concerning the increasing removal levels during oxidation of the acid yellow 36 azo dye for the Fenton type and photo-Fenton type processes (using a Ir-Sn-Sb oxide anode for the *in situ* electrogeneration of active chlorine species) were obtained by Aguilar et al. [22].

3.2. Assessment of the HOCl/UVC process using low power lamps

As the Fenton type and photo-Fenton type processes, the HOCl/UVC process is based on homogeneous catalysis reaction mediated by HO·, which is generated from homolysis of HOCl by UVC radiation (particularly the emission line at 254 nm) instead of Fe^{2+} ions in the first two processes. Recently, Sánchez-Montes et al. [30] showed that the HOCl/UVC process can be successfully used to mineralize tebuthiuron herbicide with a 9 W UVC power lamp. Therefore, in this work, a comparison between a 9 W and 5 W UVC lamps was carried out to oxidize and mineralize PCL herbicide. As can be observed in Fig. 3a, complete

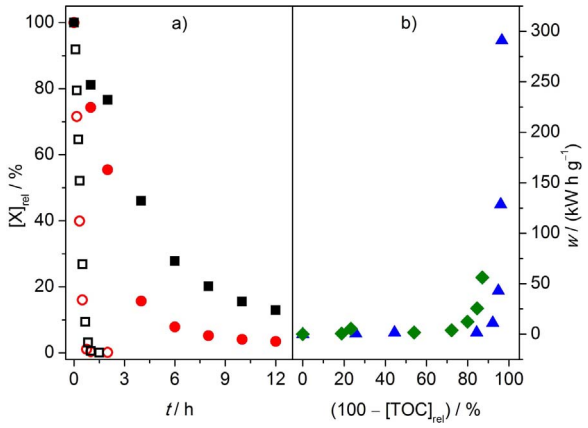

Fig. 3. a) Relative percentage decay of PCL (empty symbols) and TOC (full symbols) as a function of treatment time for the HOCl/UVC process using a (■, □) 5 W and (●,○) 9 W UVC power lamp and b) energy consumption per unit mass of removed TOC (w) as a function of TOC removal (100–$[TOC]_{rel}$) for the HOCl/UVC process using a (◆) 5 W and (▲) 9 W UVC lamp. Conditions: 20 mA cm^{-2}, pH 3, 2 g L^{-1} NaCl, and at 25 °C. A DSA® anode was used to electrogenerate active chlorine species.

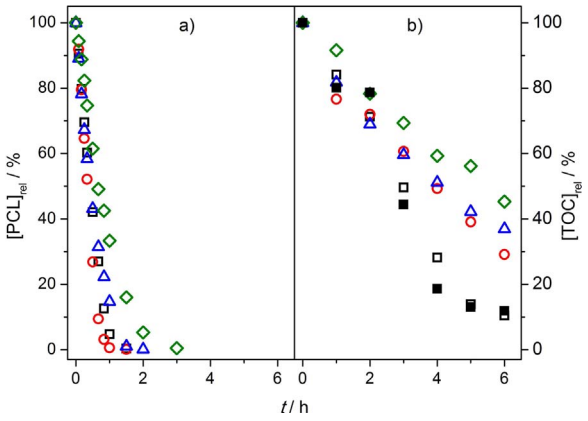

Fig. 4. Relative percentage decay of a) PCL ($[PCL]_{rel}$) and b) TOC ($[TOC]_{rel}$) as a function of treatment time for the HOCl/UVC process (using a 5 W UVC light and a DSA® anode to electrogenerate active chlorine species) at varying solution pH: (◯) 3, (△) 7, (◇) 11, and (□ and ■, the last one only for TOC decay) without pH control. Conditions: 20 mA cm^{-2}, 2 g L^{-1} NaCl at 25 °C.

oxidation of PCL was achieved after 1 h of treatment using both UVC lamps (5 and 9 W) and with similar oxidation rates (3.4×10^{-2} min^{-1} and 4.7×10^{-2} min^{-1} for the 5 and 9 W UVC power lamps, respectively.). On the other hand, the mineralization level and rate (3.3×10^{-3} min^{-1} and 5.8×10^{-3} min^{-1} for the 5 and 9 W UVC power lamps, respectively) of PCL are higher when using the 9 W lamp probably due to its slightly higher fluency rate [47] (see Table SM-1), since the conversion to CO_2 is dependent on the HO· concentration that is formed from the HOCl homolysis. For the organic load removal, only the produced HO· are effective to mineralize PCL and its intermediates, so low removal rates are expected in comparison to PCL removal. When the energy consumption of Fig. 3b is analyzed, the HOCl/UVC process using a 5 W power lamp seems to be more advantageous as the residual organic load (mainly carboxylic acids, as discussed later) is recalcitrant and requires an increasing amount of electric energy that is higher when using a 9 W UVC lamp. The obtained values of φ and *MCE* (see Fig. SM-9) using a 5 W and 9 W were also similar with an almost complete conversion of intermediates to CO_2 after 12 h of treatment. All these features confirm that the HOCl/UVC method using a 5 W UVC lamp might be sufficient to attain complete conversion of pollutants to CO_2, even in comparison to the Fenton type and photo-Fenton type processes. The synergism of the HOCl/UVC process for the TOC removal is due to the homolysis of the HOCl species to produce HO· in the solution bulk, which can be clearly seen by comparison of the summation curve of the electrochemical and photochemical methods with the experimental one using the HOCl/UVC process, as showed in Fig. SM-10. The decrease of the active chlorine concentration (calculated as Cl_2 species by a iodometric titration – see Fig. SM-11) and the similar achieved plateau when using a 5 W or 9 W UVC light confirm that the 254 nm emission line is responsible for the homolysis of the HOCl species and that the use of a 5 W lamp is sufficient to attain the highest removal rates of organics. More evidence of the production of HO· by the HOCl/UVC process can be seen in Fig. SM-2c, which shows the evolution of salicylic acid during treatment of a solution containing benzoic acid. Thus, the homolysis reaction of HOCl mediated by UVC irradiation is more efficient towards mineralization of organic contaminants than the Fenton type and photo-Fenton type based reactions. As also discussed in the work of Folkes et al. [19], the one electron reaction of HOCl and Fe^{2+} ion may lead to other reactive oxygen species that could have resulted in low oxidation and mineralization rates of the Fenton type and photo-Fenton type processes than the HOCl/UVC process.

3.2.1. *Influence of the solution pH and NaCl concentration*

The removal efficiency of organic pollutants using the HOCl/UVC process is mainly dependent on the solution pH and NaCl concentration, as these parameters are related to the distinct active chlorine species in solution (mainly HOCl and OCl^-) and their concentration, respectively. Therefore, the effect of the solution pH on the oxidation and mineralization of PCL compound was carried out using a 5 W UVC light with *in situ* electrogenerated active chlorine species, as showed in Fig. 4. Clearly, the oxidation rates attained (see Table SM-3) decreased from acidic/neutral solutions to alkaline solutions. The pH of the solution assigned as "without pH control" ranged from 7.7 (before the electrolysis) to 4.0 (after 6 h). The low removal rate of PCL in alkaline solutions is due to the presence of the OCl^- species, which has a low quantum efficiency for the homolysis reaction under UVC irradiation [47]. In addition, OCl^- may also consume the produced HO· with a higher rate than the HOCl species (scavenge reactions), as reported by Wang et al. [48]. The TOC removal rates and levels exhibited a similar trend with respect to the solution pH; however, almost complete conversion of PCL and its intermediates to CO_2 was only attained when the solution pH was not adjusted. As can be observed in Fig. 4b, that behavior is reproducible and might be related to distinct intermediate compounds generated (currently under investigation) during treatment. All these findings are in agreement with a previous work of our group [30].

As the concentration of the electrogenerated active chlorine species for the HOCl/UVC process are dependent on the NaCl concentration, assessment of the oxidation and mineralization of the PCL compound was also carried out at distinct values of NaCl concentration and in its absence using a 5 W UVC light, as showed in Fig. 5. Despite the lower removal rates attained for the conversion to CO_2 in comparison to the oxidation rates of PCL (see Table SM-4) in the presence of Cl^- ions, which is related to the different chemical modifications on the PCL molecule, the use of low NaCl concentrations (1 g L^{-1}) is sufficient to attain similar oxidation and mineralization levels among the investigated range. In the absence of Cl^- ions, complete oxidation of PCL was only achieved after 6 h of treatment, whereas ~20% of conversion to CO_2 was obtained in the same period of time. Thus, the use of Cl^- ions is essential to attain appreciable mineralization rates and levels of organics due to the electrogeneration of HOCl and its further homolysis by UVC irradiation to produce HO• species. The obtained values for the extent of combustion (φ) close to 1 after 6 h of treatment and the higher *MCE* values throughout the HOCl/UVC treatment process (see Fig. SM-12) corroborate to the importance of using NaCl, but at a lower concentration (1 g L^{-1}).

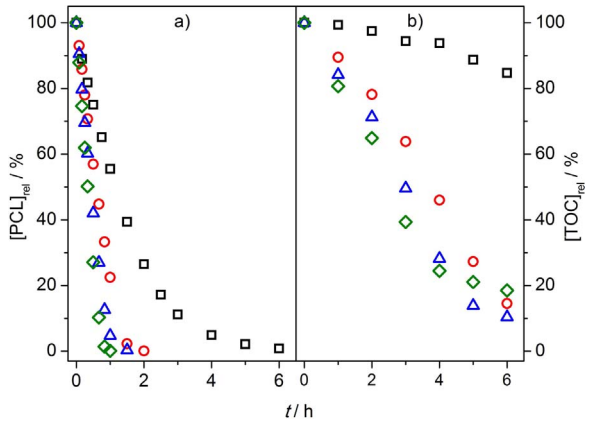

Fig. 5. Relative percentage decay of a) PCL ($[PCL]_{rel}$) and b) TOC ($[TOC]_{rel}$) as a function of treatment time for the HOCl/UVC process (using a 5 W UVC light and a DSA® anode to electrogenerate active chlorine species) at varying NaCl concentration: (□) 0.0, (○) 1.0, (△) 2.0, (◇) 4.0 g L^{-1}. Conditions: 20 mA cm^{-2}, without pH control at 25 °C.

3.2.2. Performance of the HOCl/UVC and electrochemical/BDD processes towards PCL degradation: identification of byproducts

The use of BDD anodes to oxidize and mineralize different types of organic pollutants using the electrochemical method and its derived processes is already known to result in high organic removal rates and energy efficiencies if hydrodynamic settings are properly used [49–51]. Consequently, a comparison of the electrochemical (using a BDD anode and without UVC irradiation) and HOCl/UVC processes towards oxidation and mineralization of PCL were also carried out in the optimized conditions of the HOCl/UVC process (1.0 g L^{-1} NaCl, 25 °C, no pH control), as shown in Fig. 6a, and taking into account the same surface to volume ratio and flow velocity (see Section 2.2) of the filter press flow cells. Complete oxidation of the PCL herbicide was attained after 120 min (~0.9 kA h m^{-3}) and 180 min (~1.4 kA h m^{-3}) for the HOCl/UVC and electrochemical/BDD processes, respectively. Thus, a slightly higher oxidation rate was attained when using the HOCl/UVC process (2.2×10^{-2} min^{-1}; $R^2 = 0.99$) in comparison to the electrochemical/BDD (1.3×10^{-2} min^{-1}; $R^2 = 0.97$) process. When conversion to CO_2 is analyzed, it can be observed that the HOCl/UVC process lead to ~95% of TOC removal after 12 h treatment (~6 kA h m^{-3}) than ~88% of TOC removal using the electrochemical/BDD method. The calculated CO_2 conversion rates for the HOCl/UVC and electrochemical/BDD processes remained around 4.9×10^{-3} min^{-1} ($R^2 = 0.97$) and 2.9×10^{-3} min^{-1} ($R^2 = 0.99$), respectively. In the final stage of the mineralization reaction using the HOCl/UVC process, the observed residual organic load is due to the generated carboxylic acid byproducts, as discussed below. As the mineralization reaction rate was higher for the HOCl/UVC process, the extent of total combustion (φ) for this process (0.93 after 12 h) was also superior than the one for the electrochemical/BDD method (0.88), as shown in Fig. 6b. The main difference between the HOCl/UVC and electrochemical/BDD processes is the UVC irradiation. This step led to the HOCl homolysis reaction with production of the HO· species in the solution bulk (see Fig. SM-2c). As can be observed in Fig. 6, the obtained results are quite reproducible. A comparison between the HOCl/UVC and the electrochemical/BDD processes in the presence and absence of Cl^- ions during oxidation and mineralization of PCL can be seen in Fig. SM-13. As expected, high oxidation rates were attained in the presence of Cl^- ions for both methods; however, no significant difference was observed during conversion of PCL to CO_2 using the electrochemical/BDD process in the presence or absence of Cl^- ions. Concerning the HOCl/UVC process, the use of Cl^- ions is of extreme importance to result in almost complete mineralization of PCL, as the electrogenerated HOCl species are the source of HO· mediated by UVC light. These radical species are responsible for the conversion of PCL to CO_2.

The mineralization current efficiencies (*MCE*) for the HOCl/UVC and electrochemical/BDD processes were similar and reproducible during mineralization of the PCL compound and exhibited the expected behavior of diminishment with the applied electric charge as the organic load is converted to CO_2, as showed in Fig. 7a. The evolution of the energy consumption per unit mass of removed TOC (*w*) remained close and in the range of 4–8 kW h g^{-1} for the HOCl/UVC and electrochemical/BDD treatment processes, respectively, during removal of the TOC content, as showed in Fig. 7b. That behavior is very interesting as the *w* values for the HOCl/UVC process were carried out considering the electric energy required by the UVC lamp. The electric energy used for the photochemical method was compensated by the increased cell voltage (~2 V on average) when the electrochemical method using a BDD anode, in comparison to a DSA®, was carried out. In addition, the energy consumption per unit mass of oxidized PCL was also lower for the HOCl/UVC (0.04 kW h g^{-1}) in comparison to the electrochemical/BDD (0.1 kW h g^{-1}), after complete oxidation. Therefore, the HOCl/UVC process is an interesting option as an advanced oxidation process

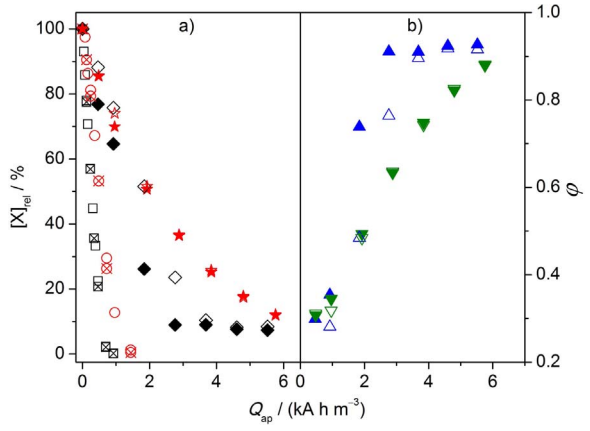

Fig. 6. a) Relative percentage decay of PCL (□, ⊠, ○, ⊗) and TOC (◊, ♦, ★, ★) as a function of the applied electric charge per unit volume of treated solution (Q_{ap}) using the HOCl/UVC (black symbols) and electrochemical (red symbols) processes and b) extent of combustion (φ) as a function of Q_{ap} for the HOCl/UVC (▲, △) and electrochemical (▼, ▽) processes. Conditions: 20 mA cm^{-2}, 1.0 g L^{-1} NaCl, without pH control at 25 °C. A DSA® anode and a 5 W UVC light were used in the HOCl/UVC process and only a BDD anode was used during the electrochemical treatment. The ⊠, ⊗, ◊, ★, ▲ and ▼ symbols refer to the experiments that were repeated. (For interpretation of the references to colour in this figure legend, the reader is referred to the web version of this article.)

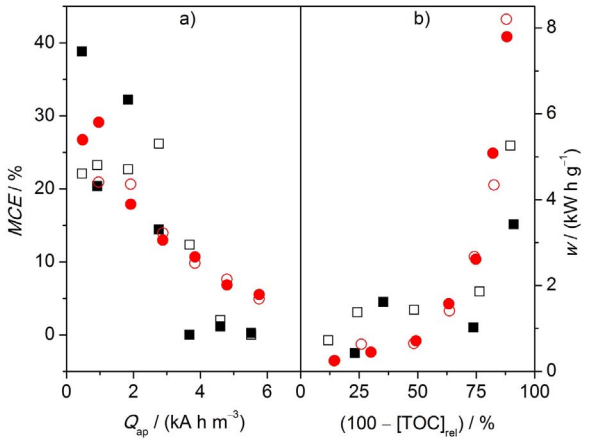

Fig. 7. a) Mineralization current efficiency (*MCE*) as a function of the applied electric charge per unit volume of treated solution (Q_{ap}) and b) energy consumption per unit mass of removed TOC (*w*) as a function of TOC removal (100–$[TOC]_{rel}$) for the HOCl/UVC (■, □) and electrochemical (●, ○) processes. Conditions: 20 mA cm^{-2}, 1.0 g L^{-1} NaCl, without pH control at 25 °C. A DSA® anode and a 5 W UVC light were used in the HOCl/UVC process and only a BDD anode was used during the electrochemical treatment. Empty symbols refer to the experiments that were repeated.

Table 1
LC–MS/MS data of the main detected byproducts during treatment of the picloram herbicide containing solution using the HOCl/UVC process.

Molar mass/(Da)	Retention time/min	Molecular ion $[M+H]^+/m/z$	Main fragment ions/m/z	Proposed chemical structure
240	8.1	241	223, 213, 195, 177, and 141	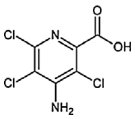
225	9.0	226	208 and 180	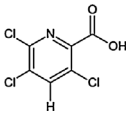
222	6.7	223	205 and 195	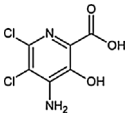

Conditions: 20 mA cm^{-2}, 1.0 g L^{-1} NaCl, without pH control at 25 °C. A DSA® anode (to electrogenerate active chlorine) and a 5 W UVC light were used in the HOCl/UVC process.

to mineralize organic pollutants.

Identification of the main produced oxidation byproducts during treatment of the PCL compound using the HOCl/UVC process were carried out by LC–MS/MS analyses. As showed in Table 1, only two intermediate compounds were detected: one of them resulting from removal of an amine group (m/z 226) and the other resulting from removal of a chlorine ion followed by a hydroxylation addition reaction (m/z 223). These intermediate compounds are in agreement with those found in the work of Abramović et al. [31], in which the mineralization of PCL herbicide was carried out using a heterogeneous photocatalytic process with TiO_2 as a catalyst with two distinct morphologies. Other intermediate compounds were detected, but their intensities were too low to perform a MS/MS analysis. In addition, no intermediate compound resulting from the rupture of the pyridine ring was observed. The fragmentation route of these two intermediate compounds, as well as the one for the parent compound, can be seen in Fig SM-14 to SM-16. Concerning the short chain carboxylic acids, only dichloroacetic (DCA) and oxamic acids were detected when using the HOCl/UVC process to mineralize the PCL molecule, as showed in Fig. 8. For the electrochemical/BDD method, other carboxylic acids were also detected such as: glyoxylic, chloroacetic, acetic, and maleic acids. The concentration evolution of these carboxylic acids as a function of treatment time can

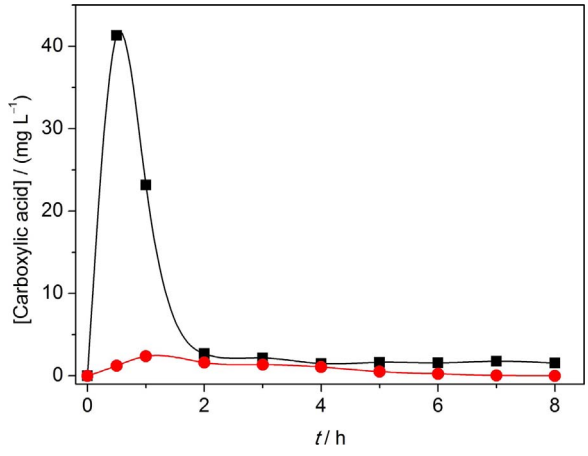

Fig. 8. Concentration evolution of the main detected carboxylic acids as a function of the treatment time (t) for the HOCl/UVC process (using a DSA® as anode to electrogenerate active chlorine species and a 5 W UVC light): (■) dichloroacetic and (●) oxamic acids. Conditions: 20 mA cm^{-2}, 1.0 g L^{-1} NaCl, without pH control at 25 °C.

be seen in Fig. SM-17, in the supplementary material file. The DCA compound (limit of quantification = 31.2 μg L^{-1}) seems to remain even after 8 h of treatment using the HOCl/UVC process and after 12 h using the electrochemical/BDD process. Chlorinated acids were produced probably due to reactions involving Cl· species, especially with aliphatic groups [52]. On the other hand, the recalcitrant oxamic acid was completely removed using both methods of treatment after 8 h. The concentration evolution of NH_4^+ and NO_3^- ions can be seen in Fig. SM-18. Considering the HOCl/UVC process, the concentration of NH_4^+ decreased throughout treatment and NO_3^- ion concentration increased until its maximum concentration (~45 mg L^{-1}) was attained. This value is close to the theoretical one (~51 mg L^{-1}, taking into account the stoichiometry of Eq. (2)) and also suggests that PCL was converted to CO_2. A similar behavior was observed for the electrochemical/BDD process, except for the lower values of NO_3^- ion concentration. In both cases, the measured concentration of NO_3^- ions was always higher than the NH_4^+ ions.

Finally, and comparing all tested methods, the HOCl/UVC process using a commercial DSA® anode to electrogenerate *in situ* active chlorine species is an interesting option to treat solutions contaminated with organic pollutants, as it can be used from acidic to neutral solutions without additions of Fe^{2+} ions.

4. Conclusions

Four different methods based on three catalytic reactions to produce HO· for mineralization of picloram herbicide were assessed in this work: HOCl/Fe^{2+} (Fenton type), HOCl/Fe^{2+}/UVA (photo-Fenton type), HOCl/UVC, and electrochemical. The process based on the Fenton type reaction with *in situ* electrogenerated HOCl species, using a commercial DSA® anode, seemed to result in a significant improvement of the mineralization removal level of picloram. Further increases were obtained when a photo-Fenton type process was employed due to the use of an UVA lamp and a consequent recovery of Fe^{2+} ions, by elimination of its complexes with H_2O and carboxylic acids. Concerning the HOCl/UVC process, almost complete mineralization of the picloram herbicide was attained within 12 h of treatment from neutral to acidic solutions, with high extent of combustion and low energy consumption, using a 5 or 9 W UVC lamp than the Fenton type and photo-Fenton type processes. When the HOCl/UVC process using a 5 W UVC lamp was compared to the electrochemical method using a boron-doped diamond (electrochemical/BDD) anode, considering the same hydrodynamic parameters of both systems, higher oxidation and mineralization rates were obtained for the HOCl/UVC process, as well as high extent of total combustion (~0.9) and low energy consumption (~4 kW h g^{-1} in comparison to ~8 kW h g^{-1} for the electrochemical/BDD method at 90% removal of TOC). Almost all intermediate compounds (two of them resulting from removal of the amine and chlorine groups) were eliminated during treatment of picloram using the HOCl/UVC process, with the exception of the dichloroacetic acid. Finally, the HOCl/UVC process based on the homolysis reaction of HOCl species to produce HO· is an interesting option to circumvent problems associated with the Fenton based (acidic solution, Fe^{2+} ion recovery, and generation of H_2O_2) and electrochemical/BDD (mass transport) processes.

Acknowledgements

São Paulo Research Foundation (FAPESP – grant number 2008/10449-7), CAPES, and CNPq are gratefully acknowledged for financial support and scholarships. We gratefully acknowledge Professors Romeu C. Rocha-Filho, Sonia R. Biaggio, Nerilso Bocchi, and Luís A. M. Ruotolo for granting access to different apparatuses. Drs. Ana Rita de Araujo Nogueira and Silvia Helena Govoni Brondi from Embrapa Pecuária Sudeste are acknowledged for access to the ion chromatograph. ADAMA Brasil and De Nora Brasil Ltda are also gratefully acknowledged for supplying samples of the picloram compound and DSA®

electrodes, respectively.

Appendix A. Supplementary data

Supplementary data associated with this article can be found, in the online version, at https://doi.org/10.1016/j.apcatb.2017.12.072.

References

[1] J.A. Luque-Espinar, N. Navas, M. Chica-Olmo, S. Cantarero-Malagón, L. Chica-Rivas, Seasonal occurrence and distribution of a group of ECs in the water resources of Granada city metropolitan areas (South of Spain): pollution of raw drinking water, J. Hydrol. 531 (Part 3) (2015) 612–625.

[2] J.-J. Jiang, C.-L. Lee, M.-D. Fang, Emerging organic contaminants in coastal waters: anthropogenic impact, environmental release and ecological risk, Mar. Pollut. Bull. 85 (2014) 391–399.

[3] J. Gomes, R. Costa, R.M. Quinta-Ferreira, R.C. Martins, Application of ozonation for pharmaceuticals and personal care products removal from water, Sci. Total Environ. 586 (2017) 265–283.

[4] Y. Luo, W. Guo, H.H. Ngo, L.D. Nghiem, F.I. Hai, J. Zhang, S. Liang, X.C. Wang, A review on the occurrence of micropollutants in the aquatic environment and their fate and removal during wastewater treatment, Sci. Total Environ. 473–474 (2014) 619–641.

[5] M. Gavrilescu, K. Demnerová, J. Aamand, S. Agathos, F. Fava, Emerging pollutants in the environment: present and future challenges in biomonitoring, ecological risks and bioremediation, New Biotechnol. 32 (2015) 147–156.

[6] H.-Q. Liu, J.C.W. Lam, W.-W. Li, H.-Q. Yu, P.K.S. Lam, Spatial distribution and removal performance of pharmaceuticals in municipal wastewater treatment plants in China, Sci. Total Environ. 586 (2017) 1162–1169.

[7] B. Díaz-Garduño, M.G. Pintado-Herrera, M. Biel-Maeso, J.J. Rueda-Márquez, P.A. Lara-Martín, J.A. Perales, M.A. Manzano, C. Garrido-Pérez, M.L. Martín-Díaz, Environmental risk assessment of effluents as a whole emerging contaminant: efficiency of alternative tertiary treatments for wastewater depuration, Water Res. 119 (2017) 136–149.

[8] J.M. Aquino, G.F. Pereira, R.C. Rocha-Filho, N. Bocchi, S.R. Biaggio, Combined coagulation and electrochemical process to treat and detoxify a real textile effluent, Water Air Soil Pollut. 227 (2016).

[9] M. Deng, Y. Zhang, X. Quan, C. Na, S. Chen, W. Liu, S. Han, S. Masunaga, Acute toxicity reduction and toxicity identification in pigment-contaminated wastewater during anaerobic-anoxic-oxic (A/A/O) treatment process, Chemosphere 168 (2017) 1285–1292.

[10] D.A.C. Coledam, J.M. Aquino, B.F. Silva, A.J. Silva, R.C. Rocha-Filho, Electrochemical mineralization of norfloxacin using distinct boron-doped diamond anodes in a filter-press reactor, with investigations of toxicity and oxidation by-products, Electrochim. Acta 213 (2016) 856–864.

[11] K.A. Rickman, S.P. Mezyk, Kinetics and mechanisms of sulfate radical oxidation of beta-lactam antibiotics in water, Chemosphere 81 (2010) 359–365.

[12] D.A.C. Coledam, M.M.S. Pupo, B.F. Silva, A.J. Silva, K.I.B. Eguiluz, G.R. Salazar-Banda, J.M. Aquino, Electrochemical mineralization of cephalexin using a conductive diamond anode: a mechanistic and toxicity investigation, Chemosphere 168 (2017) 638–647.

[13] W. Guo, J. Zhang, W. Li, M. Xu, S. Liu, Disruption of iron homeostasis and resultant health effects upon exposure to various environmental pollutants: a critical review, J. Environ. Sci. 34 (2015) 155–164.

[14] I. Oller, S. Malato, J.A. Sánchez-Pérez, Combination of advanced oxidation processes and biological treatments for wastewater decontamination-a review, Sci. Total Environ. 409 (2011) 4141–4166.

[15] T. Pérez, I. Sirés, E. Brillas, J.L. Nava, Solar photoelectro-Fenton flow plant modeling for the degradation of the antibiotic erythromycin in sulfate medium, Electrochim. Acta 228 (2017) 45–56.

[16] E. Brillas, C.A. Martínez-Huitle, Decontamination of wastewaters containing synthetic organic dyes by electrochemical methods. An updated review, Appl. Catal. B 166–167 (2015) 603–643.

[17] F.C. Moreira, R.A.R. Boaventura, E. Brillas, V.J.P. Vilar, Electrochemical advanced oxidation processes: a review on their application to synthetic and real wastewaters, Appl. Catal. B 202 (2017) 217–261.

[18] J. Radjenovic, D.L. Sedlak, Challenges and opportunities for electrochemical processes as next-generation technologies for the treatment of contaminated water, Environ. Sci. Technol. 49 (2015) 11292–11302.

[19] L.K. Folkes, L.P. Candeias, P. Wardman, Kinetics and mechanisms of hypochlorous acid reactions, Arch. Biochem. Biophys. 323 (1995) 120–126.

[20] N. Kishimoto, Y. Nakamura, M. Kato, H. Otsu, Effect of oxidation-reduction potential on an electrochemical Fenton-type process, Chem. Eng. J. 260 (2015) 590–595.

[21] N. Kishimoto, T. Kitamura, M. Kato, H. Otsu, Reusability of iron sludge as an iron source for the electrochemical Fenton-type process using Fe^{2+}/HOCl system, Water Res. 47 (2013) 1919–1927.

[22] Z.G. Aguilar, E. Brillas, M. Salazar, J.L. Nava, I. Sirés, Evidence of Fenton-like reaction with active chlorine during the electrocatalytic oxidation of Acid Yellow 36 azo dye with Ir-Sn-Sb oxide anode in the presence of iron ion, Appl. Catal. B 206 (2017) 44–52.

[23] L.P. Candeias, M.R. l. Stratford, P. Wardman, Formation of hydroxyl radicals on reaction of hypochlorous acid with ferrocyanide, a model iron(II) complex, Free Radical Res. 20 (1994) 241–249.

[24] N. Flores, P.L. Cabot, F. Centellas, J.A. Garrido, R.M. Rodríguez, E. Brillas, I. Sirés, 4-Hydroxyphenylacetic acid oxidation in sulfate and real olive oil mill wastewater by electrochemical advanced processes with a boron-doped diamond anode, J. Hazard. Mater. 321 (2017) 566–575.

[25] Y. Lan, C. Coetsier, C. Causserand, K. Groenen Serrano, On the role of salts for the treatment of wastewaters containing pharmaceuticals by electrochemical oxidation using a boron doped diamond anode, Electrochim. Acta 231 (2017) 309–318.

[26] J.M. Aquino, M.A. Rodrigo, R.C. Rocha-Filho, C. Sáez, P. Cañizares, Influence of the supporting electrolyte on the electrolyses of dyes with conductive-diamond anodes, Chem. Eng. J. 184 (2012) 221–227.

[27] M. Deborde, U. von Gunten, Reactions of chlorine with inorganic and organic compounds during water treatment-kinetics and mechanisms: a critical review, Wat. Res. 42 (2008) 13–51.

[28] J.M. Aquino, D.W. Miwa, M.A. Rodrigo, A.J. Motheo, Treatment of actual effluents produced in the manufacturing of atrazine by a photo-electrolytic process, Chemosphere 172 (2017) 185–192.

[29] G. Hurwitz, P. Pornwongthong, S. Mahendra, E.M.V. Hoek, Degradation of phenol by synergistic chlorine-enhanced photo-assisted electrochemical oxidation, Chem. Eng. J. 240 (2014) 235–243.

[30] I.J. Sánchez-Montes, B.F. Silva, J.M. Aquino, On the performance of a hybrid process to mineralize the herbicide tebuthiuron using a DSA® anode and UVC light: a mechanistic study, Appl. Catal. B 200 (2017) 237–245.

[31] B. Abramović, D. Šojić, V. Despotović, D. Vione, M. Pazzi, J. Csanádi, A comparative study of the activity of TiO_2 Wackherr and Degussa P25 in the photocatalytic degradation of picloram, Appl. Catal. B 105 (2011) 191–198.

[32] A. Özcan, Y. Şahin, A.S. Koparal, M.A. Oturan, Degradation of picloram by the electro-Fenton process, J. Hazard. Mater. 153 (2008) 718–727.

[33] G.F. Pereira, R.C. Rocha-Filho, N. Bocchi, S.R. Biaggio, Electrochemical degradation of the herbicide picloram using a filter-press flow reactor with a boron-doped diamond or β-PbO_2 anode, Electrochim. Acta 179 (2015) 588–598.

[34] R.R. Solís, F.J. Rivas, O. Gimeno, J.L. Pérez-Bote, Photocatalytic ozonation of clopyralid picloram and triclopyr. Kinetics, toxicity and influence of operational parameters, J. Chem. Technol. Biotechnol. 91 (2014) 51–58.

[35] A.D. Eaton, L.S. Clesceri, A.E. Greenberg, Standard Methods for the Examination of Water and Wastewater, 19th ed., United Book Press, Baltimore, 1995.

[36] E. Brillas, I. Sirés, M.A. Oturan, Electro-Fenton process and related electrochemical technologies based on Fenton's reaction chemistry, Chem. Rev. 109 (2009) 6570–6631.

[37] M.J. Martin de Vidales, M. Millán, C. Sáez, P. Cañizares, M.A. Rodrigo, What happens to inorganic nitrogen species during conductive diamond electrochemical oxidation of real wastewater? Electrochem. Commun. 67 (2016) 65–68.

[38] D.W. Miwa, G.R.P. Malpass, S.A.S. Machado, A.J. Motheo, Electrochemical degradation of carbaryl on oxide electrodes, Water Res. 40 (2006) 3281–3289.

[39] J.M. Aquino, K.N. Parra, D.W. Miwa, A.J. Motheo, Removal of phthalic acid from aqueous solution using a photo-assisted electrochemical method, J. Environ. Chem. Eng. 3 (2015) 429–435.

[40] J.M. Aquino, R.C. Rocha-Filho, N. Bocchi, S.R. Biaggio, Electrochemical degradation of the Disperse Orange 29 dye on a β-PbO_2 anode assessed by the response surface methodology, J. Environ. Chem. Eng. 1 (2013) 954–961.

[41] J.M. Aquino, R.C. Rocha-Filho, C. Sáez, P. Cañizares, M.A. Rodrigo, High efficiencies in the electrochemical oxidation of an anthraquinonic dye with conductive-diamond anodes, Environ. Sci. Pollut. Res. 21 (2014) 8442–8450.

[42] M.A. Rodrigo, P.A. Michaud, I. Duo, M. Panizza, G. Cerisola, C. Comninellis, Oxidation of 4-chlorophenol at boron-doped diamond electrode for wastewater treatment, J. Electrochem. Soc. 148 (2001) D60–D64.

[43] P. Cañizares, J. García-Gómez, I.F. de-Marcos, M.A. Rodrigo, J. Lobato, Measurement of mass-transfer coefficients by an electrochemical technique, J. Chem. Educ. 83 (2006) 1204–1207.

[44] C.R. Wilke, P. Chang, Correlation of diffusion coefficients in dilute solutions, AIChE J. 1 (1955) 264–270.

[45] E. Brillas, S. Garcia-Segura, Solar photoelectro-Fenton degradation of acid orange 7 azo dye in a solar flow plant: optimization by response surface methodology, Water Conserv. Sci. Eng. 1 (2016) 83–94.

[46] A. Wang, J. Qu, H. Liu, J. Ru, Mineralization of an azo dye acid red 14 by photoelectro-Fenton process using an activated carbon fiber cathode, Appl. Catal., B 84 (2008) 393–399.

[47] Y. Feng, D.W. Smith, J.R. Bolton, Photolysis of aqueous free chlorine species (HOCl and OCl^-) with 254 nm ultraviolet light, J. Environ. Eng. Sci. 6 (2007) 277–284.

[48] D. Wang, J.R. Bolton, R. Hofmann, Medium pressure UV combined with chlorine advanced oxidation for trichloroethylene destruction in a model water, Water Res. 46 (2012) 4677–4686.

[49] G.F. Pereira, B.F. Silva, R.V. Oliveira, D.A.C. Coledam, J.M. Aquino, R.C. Rocha-Filho, N. Bocchi, S.R. Biaggio, Comparative electrochemical degradation of the herbicide tebuthiuron using a flow cell with a boron-doped diamond anode and identifying degradation intermediates, Electrochim. Acta 247 (2017) 860–870.

[50] H. Rubí-Juárez, S. Cotillas, C. Sáez, P. Cañizares, C. Barrera-Díaz, M.A. Rodrigo, Removal of herbicide glyphosate by conductive-diamond electrochemical oxidation, Appl. Catal. B 188 (2016) 305–312.

[51] C. Ridruejo, C. Salazar, P.L. Cabot, F. Centellas, E. Brillas, I. Sirés, Electrochemical oxidation of anesthetic tetracaine in aqueous medium. Influence of the anode and matrix composition, Chem. Eng. J. 326 (2017) 811–819.

[52] L.H. Nowell, J. Hoigné, Photolysis of aqueous chlorine at sunlight and ultraviolet wavelengths – II. Hydroxyl radical production, Water Res. 26 (1992) 599–605.